

## Large Piezoelectric Effect in Pb-Free Ceramics

Wenfeng Liu<sup>1,2</sup> and Xiaobing Ren<sup>2,\*</sup>

<sup>1</sup>*Multi-disciplinary Materials Research Center and State Key Lab of Electrical Insulation and Power Equipment, Xi'an Jiaotong University, 710049, China*

<sup>2</sup>*Ferroic Physics Group, National Institute for Materials Science, Tsukuba, 305-0047, Ibaraki, Japan*  
(Received 25 July 2009; published 15 December 2009)

We report a non-Pb piezoelectric ceramic system  $\text{Ba}(\text{Ti}_{0.8}\text{Zr}_{0.2})\text{O}_3\text{-(Ba}_{0.7}\text{Ca}_{0.3})\text{TiO}_3$  which shows a surprisingly high piezoelectric coefficient of  $d_{33} \sim 620$  pC/N at optimal composition. Its phase diagram shows a morphotropic phase boundary (MPB) starting from a tricritical triple point of a cubic paraelectric phase (*C*), ferroelectric rhombohedral (*R*), and tetragonal (*T*) phases. The high piezoelectricity of the MPB compositions stems from the composition proximity of the MPB to the tricritical triple point, which leads to a nearly vanishing polarization anisotropy and thus facilitates polarization rotation between  $\langle 001 \rangle T$  and  $\langle 111 \rangle R$  states. We predict that the single-crystal form of the MPB composition of the present system may reach a giant  $d_{33} = 1500\text{--}2000$  pC/N. Our work may provide a new recipe for designing highly piezoelectric materials (both Pb-free and Pb-containing) by searching MPBs starting from a TCP.

DOI: 10.1103/PhysRevLett.103.257602

PACS numbers: 77.65.Bn, 77.80.Bh

For half a century, the PZT (lead zirconate titanate) family has been the icon of a large class of technologically important materials—piezoelectrics, which convert between mechanical stress (strain) and electrical voltage (charge) [1,2]. Despite its outstanding piezoelectric property, PZT is currently facing global restrictions due to its Pb toxicity; thus, there is an urgent need to develop a non-Pb substitute that can compete with PZT, in particular, with the most important high-end PZT (with  $d_{33} = 500\text{--}600$  pC/N) [3–6]. However, non-Pb piezoelectric ceramics generally have inferior piezoelectricity ( $d_{33} < 150$  pC/N in most cases) compared with PZT. Recently, their limit has been pushed to a higher level of  $d_{33} \sim 300$  pC/N [3] but is still halfway to the most-desired high-end PZT property. It remains a mystery why non-Pb piezoelectric materials do not exhibit very high piezoelectricity.

The basic approach to achieving high piezoelectricity is to place the composition of the material to the proximity of a composition-induced phase transition between two ferroelectric phases. Such a transition has been known as the “morphotropic phase boundary (MPB)” in the phase diagram [1,2]. The composition-induced ferro-ferro transition at MPB causes the instability of the polarization state so that the polarization direction can be easily rotated by external stress or electric field [7,8], thereby resulting in a high piezoelectricity and permittivity [9–13]. Recent studies further pointed out the importance of a field-induced critical behavior [14,15] and of the miniaturization of domains [16] due to vanishing polarization anisotropy at MPB [17,18]. Although these mechanisms of high piezoelectricity at MPB have so far been discussed mainly for Pb-based systems, there seems to be no particular reason that they are inapplicable to non-Pb systems. However, the MPB in non-Pb ferroelectric systems [3–5] exhibits sig-

nificantly lower piezoelectricity (typically  $d_{33} \sim 100\text{--}300$  pC/N) than that of Pb-based systems (300–600 pC/N) [4]. It is unclear why the MPB of non-Pb systems is “inferior” to that of the Pb-based systems from the existing theories.

We designed a non-Pb pseudobinary ferroelectric system  $\text{Ba}(\text{Zr}_{0.2}\text{Ti}_{0.8})\text{O}_3\text{-}x(\text{Ba}_{0.7}\text{Ca}_{0.3})\text{TiO}_3$ , or BZT-*x*BCT, where *x* is the molar percent of BCT. The samples were fabricated with a conventional solid-state reaction method with starting chemicals of  $\text{BaZrO}_3$  (98%),  $\text{CaCO}_3$  (99.9%),  $\text{BaCO}_3$  (99.95%), and  $\text{TiO}_2$  (99.9%). The calcining was performed at 1350 °C, and sintering was done at 1450 °C–1500 °C in air.

Figure 1(a) shows the phase diagram of this non-Pb BZT-*x*BCT system, determined by measuring dielectric permittivity ( $\epsilon$ ) versus temperature curves (*T*), a few typical ones shown in Figs. 1(b)–1(d). The structures of different phases were determined by x-ray diffractometry. The phase diagram is characterized by a MPB separating a ferroelectric *R* (BZT side) and *T* (BCT side) phases. The most important feature of the BZT-BCT system, being different from other non-Pb systems, is the existence of a *C-R-T triple point* in the phase diagram locating at  $x \sim 32\%$  and at  $T \sim 57$  °C. It is noted that the existence of *C-R-T* triple point characterizes many highly piezoelectric Pb-based systems such as PZT and PMN-PT [19].

Figures 2(a) and 2(b) reveal the composition dependence of ferroelectric, dielectric, and piezoelectric properties of this new system at room temperature (20 °C), in relation to the MPB composition BZT-50BCT (abbreviated as 50BCT hereafter), which has a  $T_c = 93$  °C. From Figs. 2(b)1, 2(b)2, 2(b)3, 2(b)4, 2(b)5, and 2(b)6, it is found that MPB composition 50BCT exhibits anomaly in all of the properties such as the highest spontaneous polarization  $P_m$  [Fig. 2(b)1], highest remnant polarization  $P_r$ ,

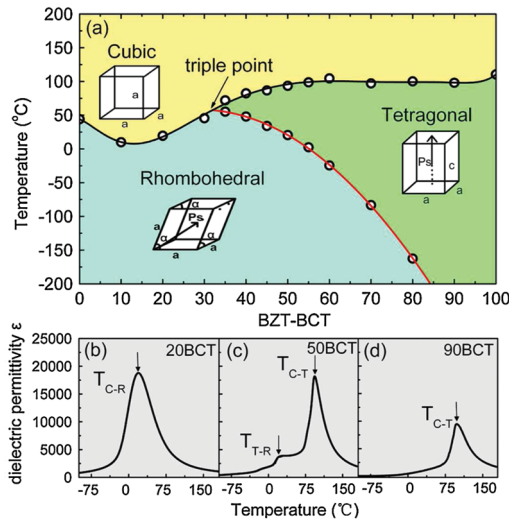


FIG. 1 (color). (a) Phase diagram of pseudobinary ferroelectric system  $\text{Ba}(\text{Zr}_{0.2}\text{Ti}_{0.8})\text{O}_3\text{-(Ba}_{0.7}\text{Ca}_{0.3})\text{TiO}_3$ , abbreviated as BZT-BCT. (b)–(d) Dielectric permittivity curves for 20BCT, 50BCT, and 90BCT, respectively.

[Fig. 2(b)2], lowest coercive field  $E_c$  [Fig. 2(b)3], and highest dielectric permittivity  $\epsilon$  [Fig. 2(b)4]. 50BCT seems to be extraordinarily “soft,” as manifested by a very low coercive field  $E_c$  of 168 V/mm and a very high permittivity  $\epsilon \sim 3060$ . The permittivity value is comparable with soft PZT materials (2000–3500) and significantly higher than other nonlead piezoelectrics (290–1740).

Figure 2(b)5 shows the most interesting result: the composition dependence of the piezoelectric coefficient  $d_{33}$ , measured by a commercial Berlingcourt-type  $d_{33}$  meter (ZJ-3A). Being consistent with the anomaly in other properties,  $d_{33}$  shows a maximum also at 50BCT, which exhibits a surprisingly high value of 560–620 pC/N depending on poling condition. This high  $d_{33}$  value even exceeds that of many soft PZTs. The  $d_{33}$  value lowers with deviating from 50BCT, but still maintains a high value of  $\sim 350$  pC/N for 45BCT and 55BCT. Figure 2(b)6 shows that 50BCT also exhibits the maximum converse piezoelectric coefficient  $dS/dE$  with a very high value of  $dS/dE = 1140$  pm/V, exceeding that of all PZT ceramics (with  $dS/dE = 360\text{--}900$  pm/V). The property anomaly at MPB of the BZT-BCT system is analogous to a similar phenomenon found in PZT and PMN-PT systems.

Figure 2(c) shows a comparison in the room temperature  $d_{33}$  of 50BCT with other non-Pb piezoelectrics and several typical PZT piezoelectrics. The  $d_{33}$  (620 pC/N) of 50BCT is about twice that the alkaline-niobate-based ceramics (currently the best non-Pb material) and several times higher than other non-Pb piezoelectrics, mostly with  $d_{33} < 150$  pC/N. When compared with the PZT family, 50BCT exhibits similar piezoelectricity with the ultrasoft PZT-5H ( $d_{33} \sim 590$  pC/N). This is unusual for a non-Pb material. Figure 2(d) shows that 50BCT (after poling) exhibits a higher electrostrain (0.057%) than the ultrasoft PZT-5H

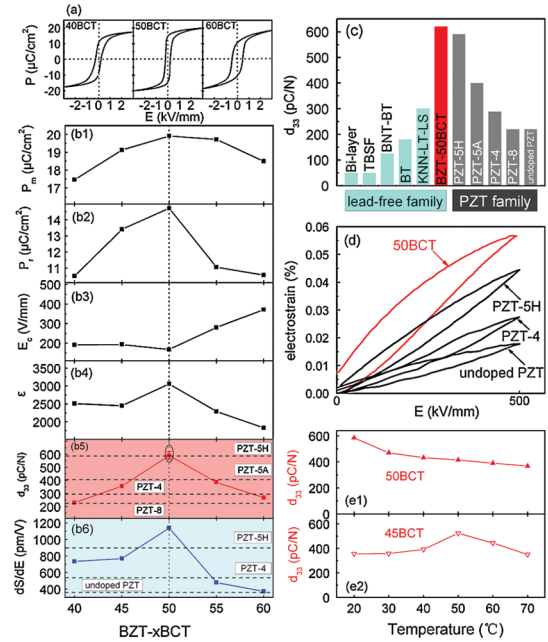


FIG. 2 (color). (a) Hysteresis loops of 40BCT, 50BCT, and 60BCT. (b1) Saturation polarization  $P_m$ , (b2) remnant polarization  $P_r$ , (b3) coercive field  $E_c$ , (b4) permittivity  $\epsilon$ , (b5) piezoelectric coefficients  $d_{33}$ , and (b6) converse piezoelectric coefficient  $dS/dE$ . Values of various PZTs are also shown as a reference. (c) Comparison of  $d_{33}$  among BZT-50BCT and other non-Pb piezoelectrics and PZT family. The non-Pb systems include Bi-layer (bismuth-layered ferroelectrics), TBSF (tungsten bronze structured ferroelectrics), BNT-BT [ $(\text{Bi}_{0.5}\text{Na}_{0.5})\text{TiO}_3\text{-BaTiO}_3$ ], BT ( $\text{BaTiO}_3$ -based ceramics), and KNN-LT-LS [(K, Na, Li)(Nb, Ta, Sb) $\text{O}_3$  ceramics]. (d) Electric-field-induced strain of BZT-50BCT in comparison with several typical PZT ceramics. (e1), (e2) show the temperature variation of  $d_{33}$  for 50BCT and 45BCT, respectively.

( $\sim 0.045\%$ ) and well exceeds unmodified PZT and PZT-4. Figures 2(e)1 and 2(e)2 show the temperature dependence of  $d_{33}$  for the MPB composition 50BCT and for an off-MPB composition 45BCT, respectively. It is found that the maximum  $d_{33}$  appears at the temperature at which the sample passes the MPB line along the temperature axis. It should be pointed out that the high  $d_{33}$  ( $\sim 620$  pC/N) of the non-Pb BZT-50BCT cannot be explained just by its relatively low  $T_c$  ( $\sim 93^\circ\text{C}$ ), because the existing non-Pb materials of similar  $T_c$  can show much lower  $d_{33}$  values [4].

As the MPB is tilted, it is possible to approach the MPB not only by changing composition, but also by changing temperature. This provides a chance to understand what happens at MPB. Figures 3(a)–3(d) show the results of *in situ* x-ray diffractometry for a 50BCT sample during cooling from its tetragonal ( $T$ ) state ( $32^\circ\text{C}$ ) through MPB state ( $14^\circ\text{C}$ ) to rhombohedral ( $R$ ) state ( $-63^\circ\text{C}$ ). The diffraction profiles at  $32^\circ\text{C}$  and  $-63^\circ\text{C}$  correspond to a tetragonal symmetry [Fig. 3(b)] and a rhombohedral symmetry [Fig. 3(d)], respectively. At the MPB state of  $14^\circ\text{C}$ ,

being close to the permittivity maximum in Fig. 3(a), the peak profiles are consistent with a superposition of  $T$  and  $R$  profiles [Fig. 3(c)]. This suggests that MPB corresponds to the coexistence of  $R$  and  $T$  phases; thus, the polarization rotation from  $\langle 001 \rangle T$  to  $\langle 111 \rangle R$  must be a first order transition.

Figure 3(e) shows that the three transitions in this system,  $C$ - $T$ ,  $C$ - $R$ , and  $T$ - $R$ , are all first order transitions, as manifested by the existence of transition hysteresis for them (see the inset). However, the hysteresis of the three first order transitions seems to gradually converge to zero at the triple point. The vanishing hysteresis for the three first order transitions at the triple point suggests that the triple point corresponds to a crossover from a discontinuous to a continuous transition and thus it is a tricritical point (TCP), which is characterized by the absence of energy barrier among the three states [20]. Figure 3(f) shows that the 30BCT, a near-tricritical composition, exhibits the highest permittivity peak at  $T_c$  compared with that of the off-triple-point compositions. This anomaly further supports that the triple point is a TCP.

With the knowledge that the triple point is a TCP, Figs. 4(a)1, 4(a)2, 4(a)3, 4(a)4, and 4(a)5 explain why the MPB of the present non-Pb system (BZT-BCT) can exhibit a very high piezoelectricity. The schematic phase diagram in Fig. 4(a)1 reproduces the key feature of the BZT-BCT system—a triple-point-type (or tricritical-type) MPB between  $T$  and  $R$  phases, which starts from a TCP. Following the approach by Rossetti *et al.* [18] and Haun *et al.* [21], the free energy ( $F$ ) of the system, being a function of composition  $x$  and temperature  $T$ , can be written as a symmetry-adapted Landau polynomial with

respect to the magnitude of polarization  $P$  and its direction (unit vector  $\mathbf{n}$ ),

$$F(x, T, \mathbf{n}, P) = A(x, T)P^2 + B(x, \mathbf{n})P^4 + C(x, \mathbf{n})P^6, \quad (1)$$

where  $A(x, T)$ ,  $B(x, \mathbf{n})$ , and  $C(x, \mathbf{n})$  are the coefficients of second, fourth, and sixth order terms, respectively. For an ideally vertical MPB starting from a TCP (i.e.,  $x_{\text{MPB}} = x_{\text{TCP}}$ ), tricriticality requires  $B(x_{\text{MPB}}, \mathbf{n}) = B(x_{\text{TCP}}, \mathbf{n}) = 0$  [20], and the equilibrium between  $T$  ( $\mathbf{n} = \langle 0, 0, 1 \rangle$ ) and  $R$  ( $\mathbf{n} = \langle 1, 1, 1 \rangle / \sqrt{3}$ ) phases demands that  $C(x_{\text{MPB}}, \mathbf{n}) = C(x_{\text{TCP}}, \mathbf{n}) = C(x_{\text{TCP}})$ . Therefore, an important conclusion can be drawn: the free energy of the MPB composition  $x_{\text{MPB}} (= x_{\text{TCP}})$  is isotropic, being independent of polarization direction. The vanishing polarization anisotropy leads to an important consequence: no energy barrier exists for polarization rotation from  $\langle 001 \rangle T$  state to  $\langle 111 \rangle R$  state [18]. This is the fundamental reason why the triple-point-type MPB has very high piezoelectric and dielectric properties.

Real MPBs are always tilted to some extent like Fig. 4(a)1, i.e.,  $x_{\text{MPB}} \neq x_{\text{TCP}}$  but  $x_{\text{MPB}} \approx x_{\text{TCP}}$ . Such a situation cannot make a zero polarization anisotropy at MPB as the above ideal case {except for the TCP [Figs. 4(a)2 and 4(a)3]}, but it can make a very weak polarization anisotropy. This weak polarization anisotropy yields a low barrier between  $\langle 001 \rangle T$  and  $\langle 111 \rangle R$  polarization states [Figs. 4(a)4 and 4(a)5], which explains the observed first order  $T$ - $R$  transition but still enables an easy polarization rotation and thus gives rise to high dielectric and piezoelectric properties. The above mechanism may also be applicable to Pb-based systems (like PZT and PMN-PT), as these systems are also characterized by a triple-point-type MPB. A rigorous modeling of the triple-point-type MPB will appear elsewhere [22].

By contrast, existing non-Pb piezoelectric systems do not seem to show a triple-point-type MPB like Fig. 4(a)1. Many of them (like alkaline niobate) show a polymorphic-type MPB, which starts from a polymorphic point of a terminal composition like Fig. 4(b)1. Polymorphic transition has also been shown to enhance piezoelectric properties by the instability with respect to polarization rotation [11]. However, unlike the triple-point situation, for a first order polymorphic transition, there is no thermodynamic restriction to the anisotropy of  $B(x, \mathbf{n}) (< 0)$  and  $C(x, \mathbf{n}) (> 0)$  terms. Thus, they are quite anisotropic along the whole polymorphic boundary line, as shown in Figs. 4(b)2, 4(b)3, 4(b)3, 4(b)4, and 4(b)5. This results in a larger energy barrier (compared with the case of triple-point MPB) between the two polarization states ( $T$  and  $O$ ). As a result, the property enhancement by polymorphic transition is not as significant as in the triple-point-type MPB systems. This can explain why such non-Pb materials have a lower piezoelectric and dielectric property compared with that of triple-point MPB systems.

Finally, it should be noted that strictly speaking high piezoelectricity not only requires a low polarization an-

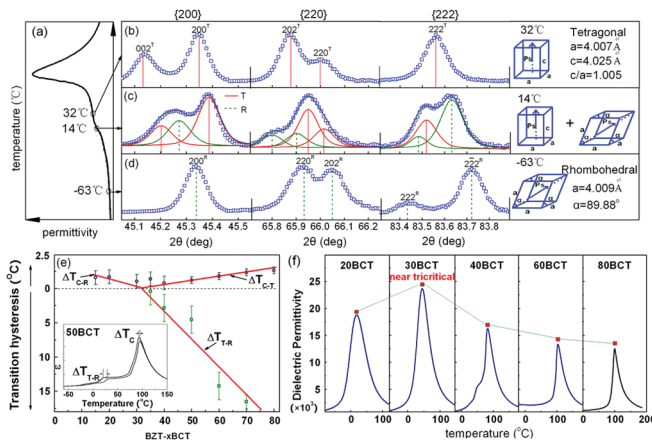


FIG. 3 (color). (a)–(d) *In situ* x-ray diffraction (XRD) profiles of 50BCT during cooling. (a) Permittivity versus temperature relation of the sample. (b) XRD profiles at 32 °C. (c) XRD profiles at 14 °C (MPB). (d) XRD profiles at –63 °C. (e) At triple point (~32BCT), the transition hysteresis (as defined in the inset) of the three first order transitions ( $C$ - $T$ ,  $C$ - $R$ , and  $T$ - $R$ ) vanishes. (f) Highest permittivity peak appears for a near-tricritical composition, 30BCT.



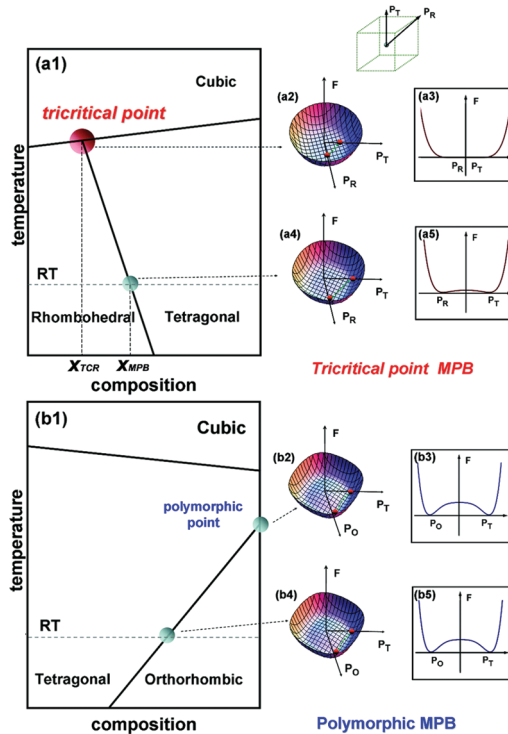


FIG. 4 (color). (a1) Schematic of a tricritical-type MPB between tetragonal ( $T$ ) and rhombohedral ( $R$ ) phases. (a2), (a3) Isotropic free energy surface for tricritical point. (a4), (a5) Nearly isotropic free energy surface of MPB composition at room temperature. (b1) Schematic of a polymorphic-type MPB between tetragonal ( $T$ ) and orthorhombic ( $O$ ) phases. (b2), (b3) Schematic anisotropic free energy surface for polymorphic point. (b4), (b5) Schematic anisotropic free energy surface for polymorphic MPB (room temperature). The 1D free energy plots in (a3), (a5) and (b3), (b5) show the free energy barrier along the polarization rotation path [from  $P_T\langle 001 \rangle$  or  $P_R\langle 111 \rangle$  (or  $P_O\langle 110 \rangle$ )].

isotropy but also a softening of the lattice [23]. Fortunately, low polarization anisotropy and elastic softening go hand in hand, both contributing to a high piezoelectricity.

In summary, we report a non-Pb piezoelectric system BZT-BCT, which exhibits a very high piezoelectric coefficient of 620 pC/N at MPB, which is comparable even with high-end PZT. The high piezoelectricity stems from an MPB starting from a triple point, which is a TCP and causes a very low energy barrier for polarization rotation and lattice distortion. Our work indicates that there is no special reason that non-Pb piezoelectric materials should always be inferior to Pb-based systems; if a suitable TCP-type MPB is designed, non-Pb systems may exhibit equally excellent or even better piezoelectricity as Pb-based ones. For the MPB composition (50BCT) of the BZT-BCT system, we predict a 3–4 times larger piezoelectricity ( $d_{33} =$

1500–2000 pC/N) in single-crystal form, similar single-crystal enhancement having been empirically known in PMN-PT [24].

The authors are grateful to D.Z. Xue, H.X. Bao, C. Zhou, and Y.M. Zhou for the contribution to Figs. 3(e), 3(f), and 4. W.F. Liu acknowledges the support of the National Natural Science Foundation of China (Grants No. 50720145101 and No. 50702042), the National Basic Research Program of China (Grants No. 2004CB619303 and No. 2010CB631003), and 111 project of China.

\*Ren.Xiaobing@nims.go.jp

- [1] K. Uchino, *Ferroelectric Devices* (Marcel Dekker, New York, 2000), Chap. 7.
- [2] B. Jaffe, *Piezoelectric Ceramics* (Academic Press, India, 1971), Chap. 7.
- [3] Y. Saito *et al.*, *Nature (London)* **432**, 84 (2004).
- [4] T.R. Shrout and S.J. Zhang, *J. Electroceram.* **19**, 113 (2007).
- [5] T. Takenaka and H. Nagata, *J. Eur. Ceram. Soc.* **25**, 2693 (2005).
- [6] X.B. Ren, *Nature Mater.* **3**, 91 (2004).
- [7] H.X. Fu and R.E. Cohen, *Nature (London)* **403**, 281 (2000).
- [8] M. Ahart *et al.*, *Nature (London)* **451**, 545 (2008).
- [9] B. Noheda *et al.*, *Phys. Rev. Lett.* **86**, 3891 (2001).
- [10] L. Bellaiche, A. Garcia, and D. Vanderbilt, *Phys. Rev. Lett.* **84**, 5427 (2000).
- [11] S. Wada *et al.*, *Jpn. J. Appl. Phys.* **38**, 5505 (1999).
- [12] R. Ahluwalia, T. Lookman, A. Saxena, and W. Cao, *Phys. Rev. B* **72**, 014112 (2005).
- [13] D. Damjanovic, *J. Am. Ceram. Soc.* **88**, 2663 (2005).
- [14] Z. Kutnjak, J. Petzelt, and R. Blinc, *Nature (London)* **441**, 956 (2006).
- [15] Z. Kutnjak, R. Blinc, and Y. Ishibashi, *Phys. Rev. B* **76**, 104102 (2007).
- [16] Y.M. Jin *et al.*, *Phys. Rev. Lett.* **91**, 197601 (2003).
- [17] Y. Ishibashi and M. Iwata, *Jpn. J. Appl. Phys.* **37**, L985 (1998).
- [18] G.A. Rossetti, A.G. Khachatryan, G. Akcay, and Y. Ni, *J. Appl. Phys.* **103**, 114113 (2008).
- [19] D.E. Cox *et al.*, *Appl. Phys. Lett.* **79**, 400 (2001).
- [20] E.K.H. Salje, *Phase Transitions in Ferroelastic and Co-Elastic Crystals* (Cambridge University Press, Cambridge, 1990).
- [21] M.J. Haun, E. Furman, S.J. Jang, and L.E. Cross, *Ferroelectrics* **99**, 13 (1989).
- [22] X.B. Ren (to be published).
- [23] M. Iwata, H. Orihara, and Y. Ishibashi, *Ferroelectrics* **266**, 57 (2002).
- [24] S.-E. Park and T.R. Shrout, *J. Appl. Phys.* **82**, 1804 (1997).